




Lineament, Qualitative Interpretation and Depth Evaluation of Potential Field Signatures in the Abeokuta Region, Southwestern Nigeria

Layade, G. O.¹  | Edunjobi, H. O.²  | Ajayi, K. D.¹ 

1. Department of Physics, College of Physical Sciences, Federal University of Agriculture, Abeokuta, Nigeria.

2. Department of Physics, Sikiru Adetona College of Education, Science and Technology, Omu-Ajose, Nigeria.

Corresponding Author E-mail: layadeoluyinka018@gmail.com

(Received: 8 May 2023, Revised: 6 June 2023, Accepted: 26 Sep 2023, Published online: 20 Feb 2024)

Abstract

Ground gravity and magnetic geophysical surveys are proven veritable tool in the imagery of the subsurface through the analyses of their responses (potential field data). This research attempts to delineate subsurface linear structures that are possible conduits for mineral accumulation at a 2,500 m² active exploration site of FUNAAB, Abeokuta region. Abeokuta is embayed in the Dahomey Basin comprising of magmatic older granites of Precambrian age to early Paleozoic age. The qualitative interpretation technique employed by visualizing the grids reveals variations in density contrasts and susceptibilities, which connote the lithological distribution of the basement. Areas of high gravity and magnetic values directly correspond to areas of high density bodies and magnetically susceptible mineral contents, respectively. While the lows and steep discontinuities of both gravity and magnetic maps predict possible entrapments of mineral accumulation in the study area. The depth evaluation techniques employed are Peter's Half Slope Method (PHSM) and 3D Euler deconvolution, showing the magnetic depths to basement range as 3.18 m to 5.88 m for PHSM and 1.00 m to 4.43 m for 3D Euler deconvolution. The gravity depth to basement reveals 7.03 m to 14.72 m for PHSM and 0.96 m to 4.13 m for 3D Euler deconvolution. The average depth results obtained clearly show that the study location is composed of shallow depth intrusive sources.

Keywords: Lineament, Potential field data, Qualitative, Peter's Half Slope Method (PHSM), Deconvolution.

1. Introduction

Delineating subsurface geologic features like faults, geologic boundaries, lineaments and fractures can be achieved through the interpretation and analysis of potential field signatures. A veritable and significant tool in predicting the composition of the underground is potential field data. Gravity and magnetic surveys are broadly categorized as potential field measurement according to Telford et al. (1976) and Layade et al. (2020), which offer appropriate approach for detecting steep discontinuities such as lineaments, faults, voids and cracks (Nabighian & Hansen, 2005; Araffa et al., 2018), as well as evaluating the depth of regolith, which is very vital to predicting certain rock formations or mineral potentials of an area of study (Edunjobi et al., 2021). Essa and Munsch (2019) used the Particle Swarm Optimization (PSO) technique to interpret the Second Moving Average (SMA)

residual gravity anomalies can be obtained from measured gravity data. Regional signals of the measured gravity data were reduced using filters of consecutive window lengths (s-values). This approach proved efficient as it helps to get rid of regional anomalies and appraise the real model parameters of buried structures. The accuracy of the technique was tested on two different theoretical examples and investigated on three real data for mineral exploration from Canada, Cuba and India. Three different least-squares minimization approaches, as designed by Abdelrahman and Essa in 2015, have been utilized to extract the parameters of buried structures from the residual anomalies of measured gravity data over the Gazal fault, south Aswan, Egypt. The results of the parameters extracted are in agreement with the actual faults and those in published articles. The method yields good results in

Cite this article: Layade, G. O., Edunjobi, H. O., & Ajayi, K. D. (2024). Lineament, Qualitative Interpretation and Depth Evaluation of Potential Field Signatures in the Abeokuta Region, Southwestern Nigeria. *Journal of the Earth and Space Physics*, 49(4), 37-55. DOI: <http://doi.org/10.22059/jesphys.2023.358877.1007525>

E-mail: (1) ajayikenny94@gmail.com (2) edunjobihazeez@gmail.com



cases where gravity anomalies are contaminated with random noise.

This research attempts to study the subsurface by delineating possible linear features such as fractures, shear zones and faults that can be potential entrapments or hosts for accumulated minerals and to serve as guides for exploration (Paterson & Reeves, 1985). This research also sets out to determine the depth to basement as a ploy to estimate the sedimentary thickness of the study area, which will help in economic decisions in the area as to the likely mineral composition of the location. The minimum sedimentary thickness for natural resources accumulation varies from place to place; for instance, a sedimentary thickness of about 2 km to 4 km is required for hydrocarbon stockpiling, on the authority of Dow (1978); Wright et al. (1985), Cornford (1990); Gluyas and Swarbrick (2005) whereas lesser sedimentary thickness can be found to contain near-surface metamorphic minerals. This research was undertaken at an active exploration site, at the Institute of Food Security, Environmental Resources and Agricultural Research (IFSERAR) in the Federal University of Agriculture, Abeokuta (FUNAAB). Upon continuous excavation of the top soil of the area, some linear trends (entrapments) were sighted, which aroused the interest on this research.

In delineating the structural features, detailed qualitative and Centre for Exploration Targeting (CET) grid analyses of the produced maps were employed to optimally observe the steep discontinuities and/or continuous elongation of contours, while 3-D Euler deconvolution method and Peter's Half-Slope Method (PHSM) were the quantitative techniques adopted in evaluating the depth to basement of potential field sources in the area. Anudu et al. (2012) analyzed aeromagnetic data over Wamba and its adjoining areas in north central Nigeria using Peter's Half Slope Method to estimate the depth of magnetic bodies. The study also highlighted the effectiveness of aeromagnetic data in mapping metalliferous mineral deposits and delineating linear trends. The ground gravity data of Ilesha and its

environs, obtained by the Nigeria Geological Survey Agency (NGSA) was interpreted qualitatively and quantitatively by Layade et al. (2020), to evaluate the depth to basement of gravity anomalous sources and map out linear structures that are potential conduits and entrapments for mineral targets.

Akinse and Gbadebo (2016) carried out a study in parts of the Abeokuta metropolis to determine the lithologic features present in the area. This study investigated the nature of the occurrence of rocks and identified the various rock types in order to produce a geological map. Edunjobi et al. (2021) used the Source Parameters Imaging and 3D-Euler deconvolution methods on an aeromagnetic dataset of Abeokuta as depth estimate techniques in the geological transition zones of Abeokuta as well as using the CET grid analysis to suggest possible transition zones and lineaments in the area.

2. Location and Geologic Setting of the Study Area

The research was carried out at an exploration site situated at the Institute of Food Security, Environmental Resources and Agricultural Research (IFSERAR) inside the Federal University of Agriculture, Abeokuta (FUNAAB). The study area shares the same geologic setting with Abeokuta, an area that comprises older granites that are magmatic and of Precambrian age to early Paleozoic age, as posited by Jones and Hockey (1964). Dahomey Basin, otherwise known as the Benin Basin embays Abeokuta, which is composed of granite, gneiss, quartzite, calcisilicate, amphibolites and biotite-hornblende schist, according to Rahaman (1976). The migmatite group (migmatite-gneiss complex) is distributed over the study area, as shown by the geological map of the study area (Figure 1). The location of the study lies approximately within latitudes 7.228669 N to 7.229121 N and longitudes 3.400536 E to 3.400988 E, covering an area of 2,500 m² with an average elevation of 140 m, inside Alabata, Abeokuta. Abeokuta is the state capital of Ogun state, and it is a part of the basement complex of the geological setting of southwest Nigeria (Obaje, 2009).

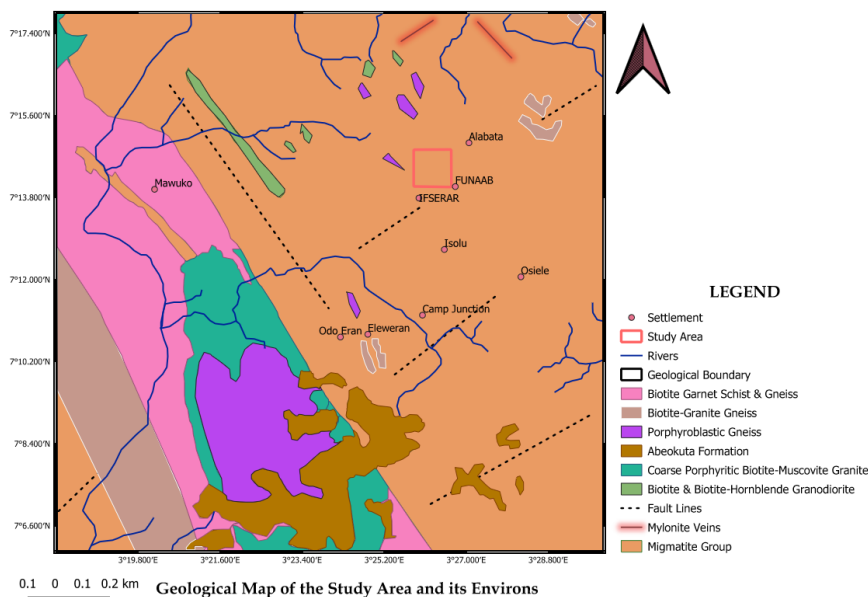


Figure 1. Geological map of the surveyed plot and its adjoining areas (modified after the geological map of Ogun state produced by NGSA in 2005).

2. Materials and Methods

Geophysical surveys of the area were taken in situ to generate corrected sets of gravity and magnetic data used in the investigation of potential sources, yielding the depth to basement of subsurface features. Listed below is the equipment used in the data acquisition.

Lacoste and Romberg Gravity Meter: It was used to measure the differences in the Earth's gravitational field at different points. The Lacoste and Romberg gravity meter, powered by 10.8 V lithium-ion batteries, was used to measure relative gravity values. This type of gravity meter is made with metal parts, which makes it more rugged than those made of fused quartz since the thermal expansion and contraction of metal are generally greater than those of quartz. This Lacoste and Romberg gravity meter (Model G) is specially designed to operate at a thermostated temperature range of 47°C to 55°C. Among its visible outer parts are nulling dial, gear box, adjustment knob/lever and an aluminum base-plate, which helps to ensure balances before taking measurements.

Magnetometer: GEM GSM-19 overhauser is a proton precession magnetometer that measures the intensity of the total field. It is robust and effective, with a high sensitivity of 0.022 nT, high resolution of 0.01 nT, an accuracy of ± 0.1 nT and an average data memory of 24,500 readings. It is designed to operate at a temperature of -40°C to 50°C. GEM GSM-19 has two sensors that make it

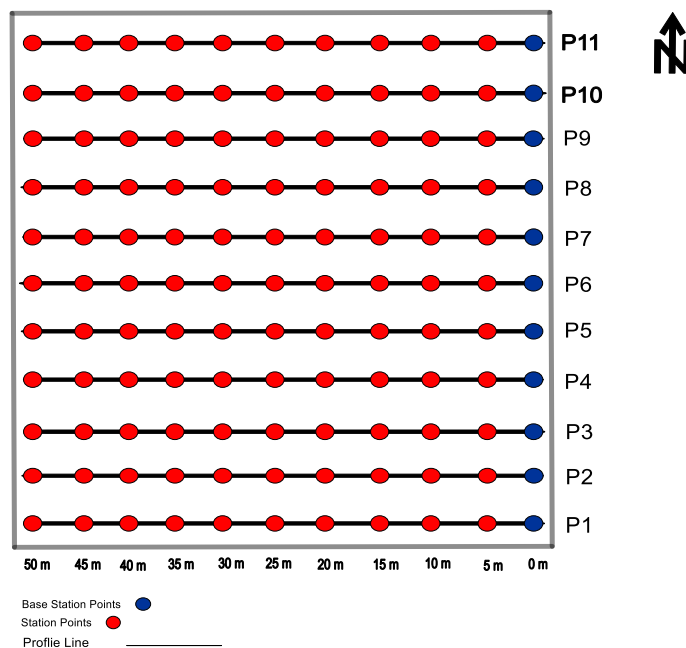
possible for the equipment to be used as gradiometer when switched to the gradiometry mode.

Global Positioning System (GPS): This instrument (Garmin handheld GPS) helped in picking the coordinates and elevation of station points as well as locating the magnetic north, which is very vital in magnetic field survey. It is a multi-channel radio navigation system, working free of internet or telephonic reception.

Other instruments or tools used are; the measuring tape to measure distances, a stopwatch to know the approximate time of surveys and readings, wooden pegs for appropriate gridding of survey plot, twine (thread) to connect station points and ensure measurements are not taken out of positions, and a data sheet for recording of values. Oasis Montaj, Surfer and Microsoft Excel worksheets are the interpretation software packages and data correction tools used.

2-1. Data Acquisition Procedure

A total number of 121 datasets for each gravity and magnetic geophysical survey were generated through the surveyed plot measuring 50 m by 50 m. There are eleven traverses (each 50 m long) across the surveyed plot at 5 m inter profile spacing from one another. The movement of the survey is in an east-west direction at 5 m along each profile. The first station point on each of the profiles is established as the base station, as illustrated by Figure 2 below.



Data Acquisition Layout for Ground Magnetism and Ground Gravity

Figure 2. Layout for the acquisition of gravity and magnetic data.

In gravity measurements, the Lacoste and Romberg meter was carefully placed in the concave aluminum base-plate and leveling was ensured by adjusting the various level knobs. The coarse and fine readings were taken three times to get an average of the readings for better accuracy. The coarse side is normally used to place the gravimeter into the operating range of the fine side. In the magnetic field survey, an average corresponding value of the total field at each point is recorded. The start and end times of measurements, elevation of station points, and latitude and longitude of points were all also recorded on the datasheet for gravity and magnetic surveys.

2-2. Data Preparation and Reductions

Data acquired on each traverse of the gravity and magnetic surveys is prepared on a Microsoft excel sheet for easy computations. The essence of data reduction or correction is to identify and remove effects by sources that are not of direct geological interest or not related to local geologic bodies. The gravity data reduction process involves computing the Bouguer Anomaly (BA) through; (i) drift correction that are caused by expansion and contraction of the survey instruments, (ii) latitude correction (g_{λ}) caused by the shape and rotation of the Earth, (iii) free Air Correction (FAC) that accounts for gravity variations due to the elevation difference; and

(iv) Bouguer Correction (BC) that is the removal of excess mass (rocks) underlying the measured point and above the reference datum (i.e. geoid). This reduction procedure is adapted from Adejuwon *et al.* (2018).

$$BA = g_{obs} - g_{\lambda} + FAC - BC \quad (1)$$

In reducing the ground magnetic data, station drift that equals the ratio of change in base station to change in survey time, was used to obtain the resultant field, which was then plotted against survey intervals on the Microsoft Excel in order to remove the regional field by an approach known as the linear trend analysis that involves the least square fitting technique, as explained by Joshua *et al.* (2017). The regional field is subtracted from the observed field to have a resultant residual anomaly field that consequently represents the distribution of magnetic anomalies across the field.

2-3. Qualitative Interpretation and Lineament Extraction

The obtained Bouguer anomalies and measured intensities of the total field are prepared and gridded using the minimum curvature algorithm described by Edunjobi *et al.* (2021), Webring (1981), with a grid cell size of 5 m, to produce the Bouguer Gravity Field (BGF) and the Total Magnetic Intensity (TMI) maps presented as Figure 3 and Figure 4, respectively.

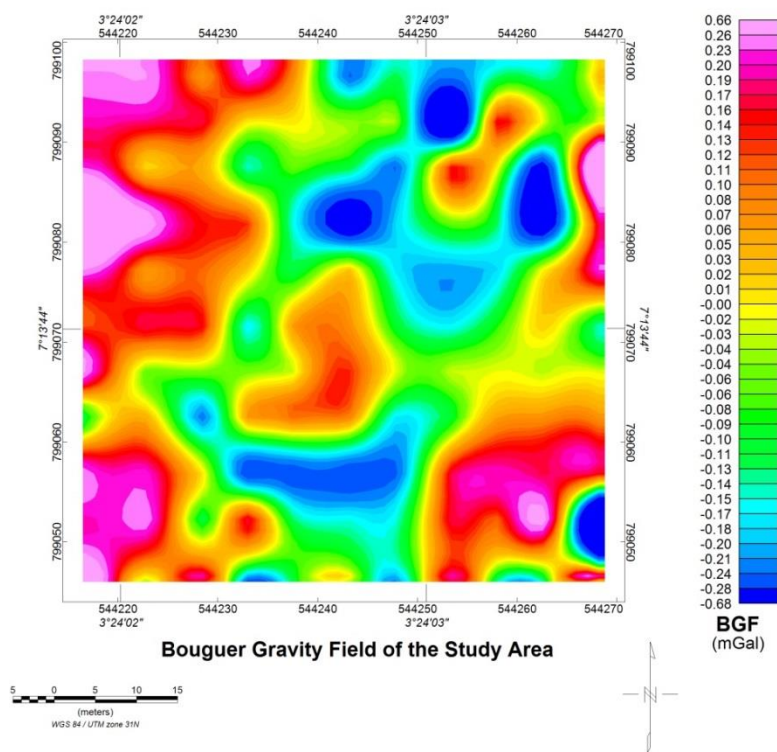


Figure 3. Bouguer Gravity Field (BGF) Map representing the total gravity field.

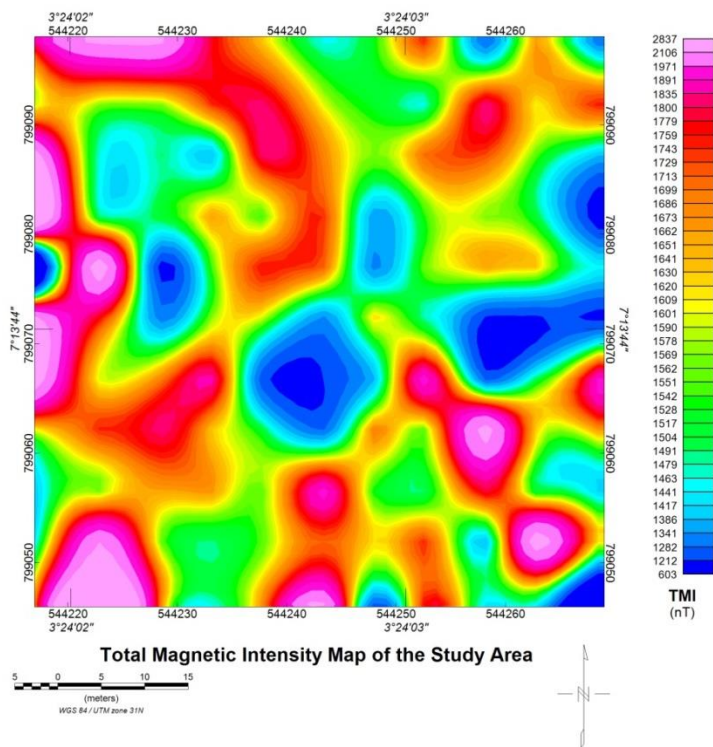


Figure 4. Total Magnetic Intensity (TMI) Map representing the total magnetic field.

The choice of a 5 m grid interval is to ensure that it agrees with station spacing on traverses, over gridding can introduce noise-to-signals according to Reid et al. (2012). These produced fields are representatives of the gravity and magnetic fields, whose

spectra and its depth estimates are shown in Figures 5 and 6. The power spectrum is a good pointer to understanding the behavior of potential field data, for knowing the appropriate and matching filter to apply in the data reduction.

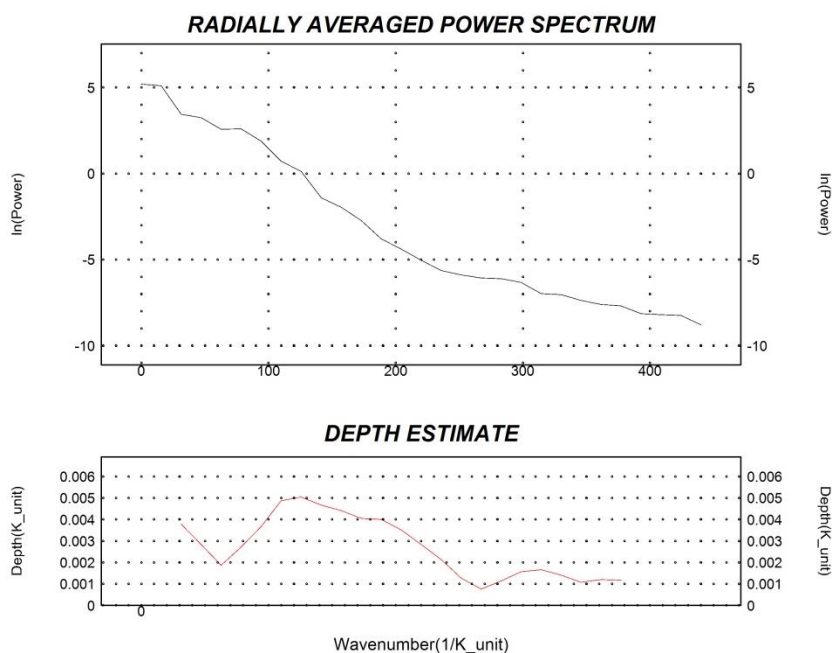


Figure 5. Radially Averaged Power Spectrum of the Gravity Field, and its Depth Estimates.

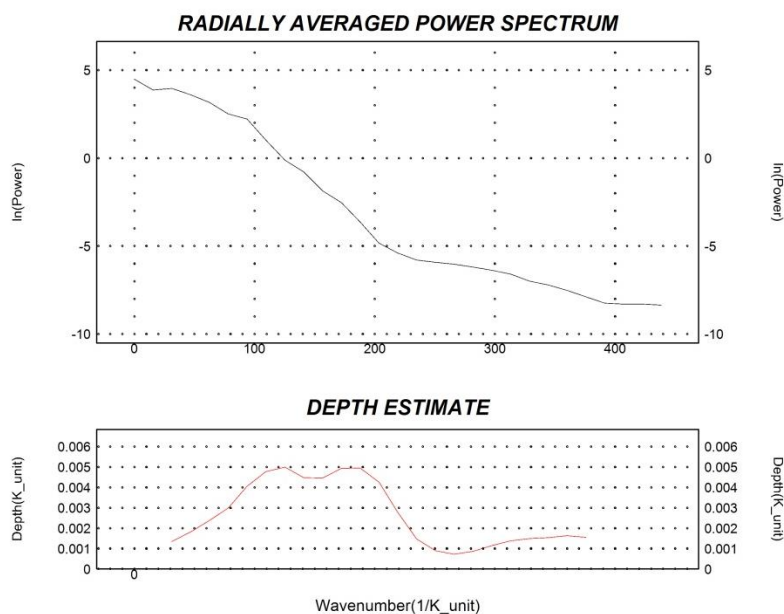


Figure 6. Radially Averaged Power Spectrum of the Magnetic Field, and its Depth Estimates.

Three segments of deep-seated (regional), intermediate (residual) and shallow (possibly noises) potential field sources can be clearly observed from both spectra. Regional-residual separation of the gravity field was achieved through the application of the Gaussian filter (High Pass filter), which helps to accentuate shallow gravity signatures, otherwise known as residual anomalies. While the residual anomalies of the magnetic

field were obtained through linear trend analysis after the regional effects were removed. The resultant residual data was gridded and contoured to represent the Residual Magnetic Intensity of the field, as shown in Figure 8. It is important to note that the spectrum plot is an effective means of filter applications, as it would suggest an appropriate filter to attenuate noises or accentuate signals.

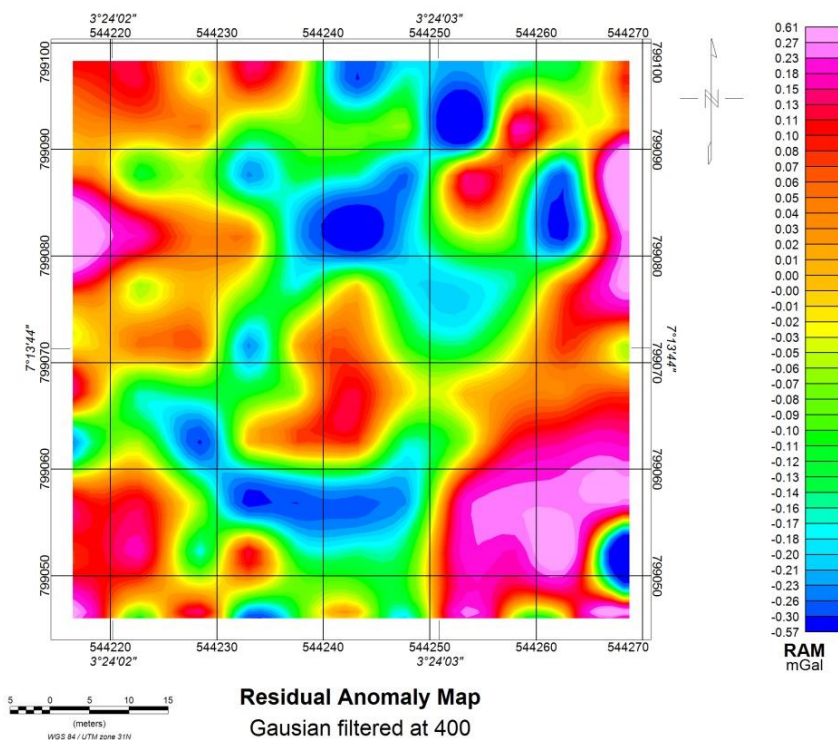


Figure 7. Residual Anomaly Map (RAM).

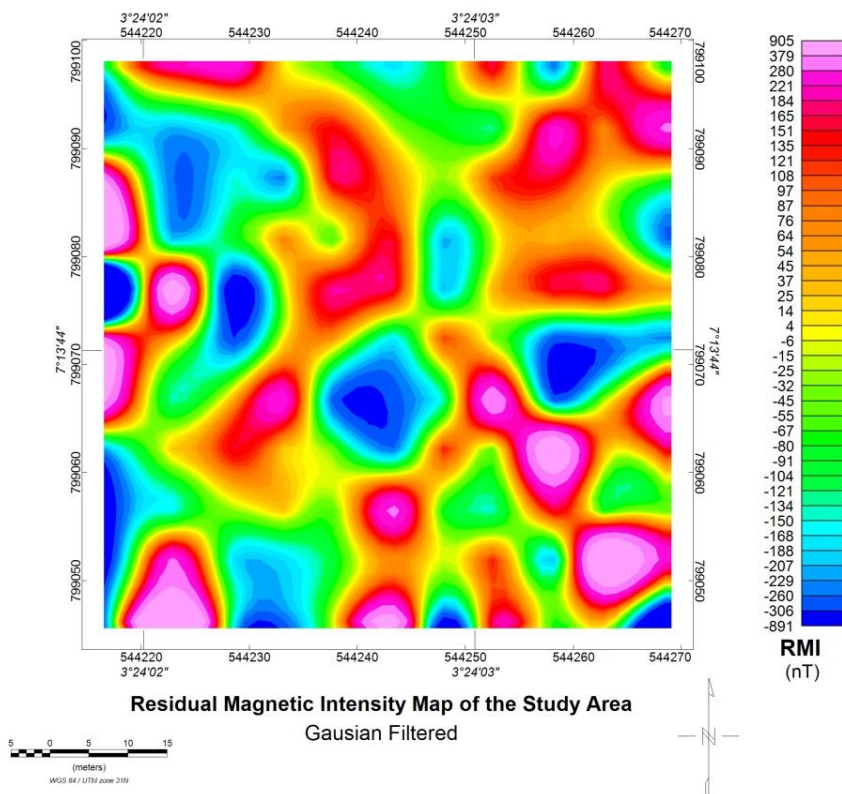


Figure 8. Residual Magnetic Intensity (RMI) Map.

The gravity and magnetic derivative components of the field were computed by applying the two-dimensional Fast Fourier Transform (2D-FFT) directional filter on short wavelength anomalies (otherwise

known as high frequency anomalies, herein referred to as the residual anomaly fields) to weaken or attenuate long wavelength anomalies associated with deeply seated anomalies (Hesham & Hesham, 2016). The x

(FHD-X) and y (FHD-Y) first horizontal derivatives, as well as z (FVD) first vertical derivative, are calculated to hone the edges of potential anomalies' signatures, according to Layade et al. (2020).

The horizontal derivative is expressed mathematically as:

$$F\left[\frac{d^n\phi}{dx,y^n}\right] = (ik_{x,y})^n F(\phi) \quad (2)$$

where;

F = Fourier transform of the potential field

$n = 1, 2$; the n^{th} order horizontal derivative

ϕ = Potential of the field

$(ik_{x,y})$ is an operator which transform a function into n^{th} order derivative with respect to either x or y.

The first vertical derivative is expressed mathematically as:

$$F\left[\frac{d^n\phi}{dz^n}\right] = k^n F(\phi) \quad (3)$$

where,

F = Fourier transform of the potential field

$n = 1, 2$, the n^{th} order vertical derivative

ϕ = Potential of the field

The total horizontal and tilt derivatives play very important roles in delineating shallow basement structures such as cracks, faults, fractures and lineaments. The total horizontal derivative is the vector sum of the x and y derivatives, while the tilt derivative is the arctan of the ratio of the vertical derivative (z) to the horizontal derivatives, (Falufosi & Osinowo, 2021). FHD-X is the first horizontal derivative of the gravity field along the X-direction presented in Figure 9, FHD-Y is the first horizontal derivative map of the magnetic field along the Y-direction shown in Figure 10. The tilt derivatives of gravity and magnetic fields are represented in Figure 11 and Figure 12, respectively.

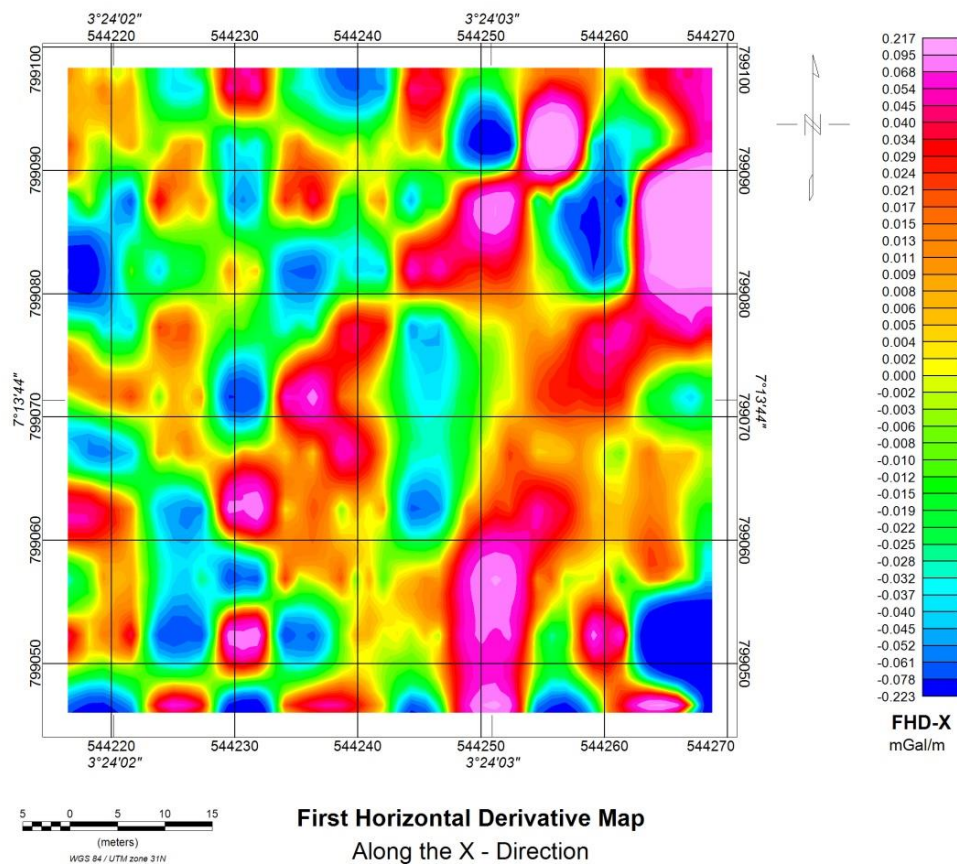


Figure 9. First horizontal derivative (along the X-direction) map of the gravity field.

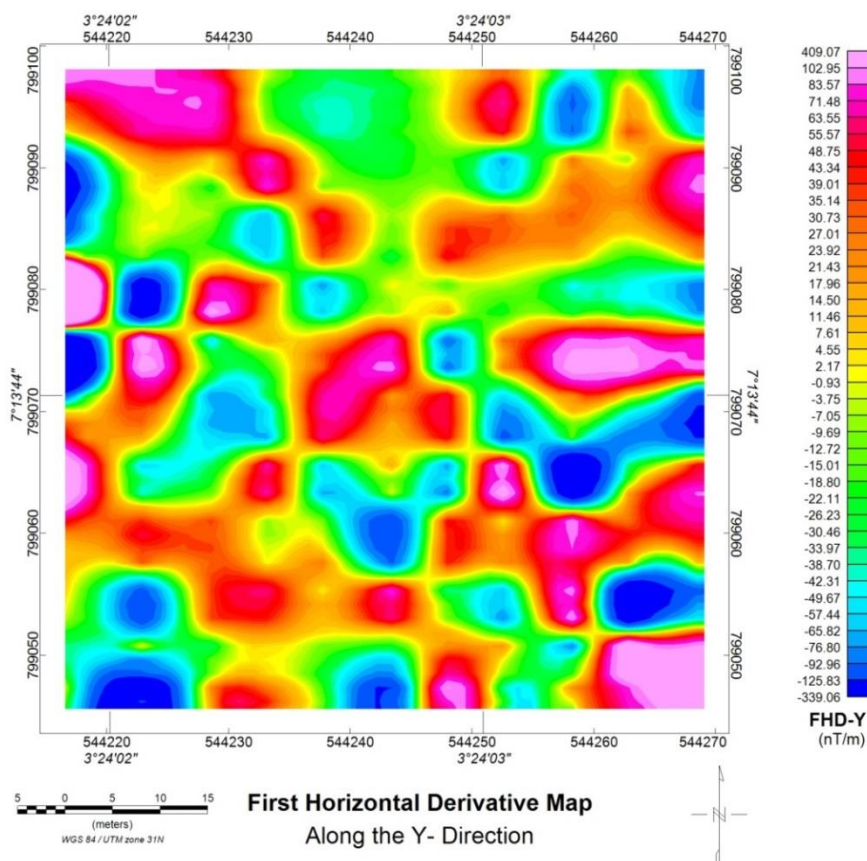


Figure 10. First horizontal derivative (along the Y-direction) map of the magnetic field.

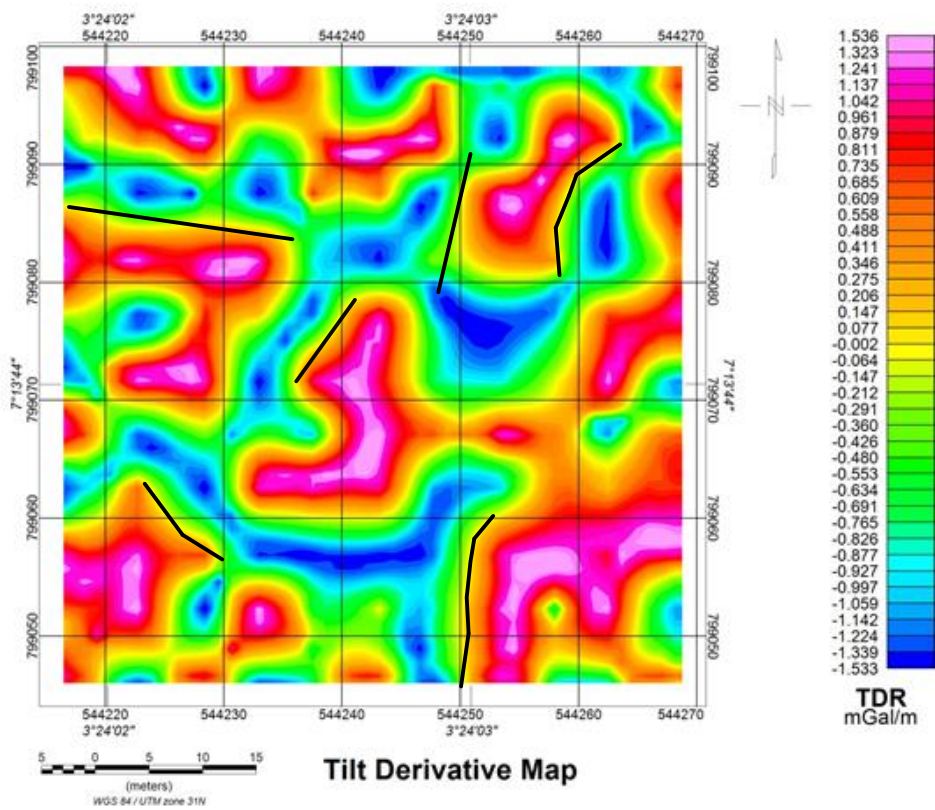


Figure 11. Tilt derivative map of the gravity field (lineament inferred map).

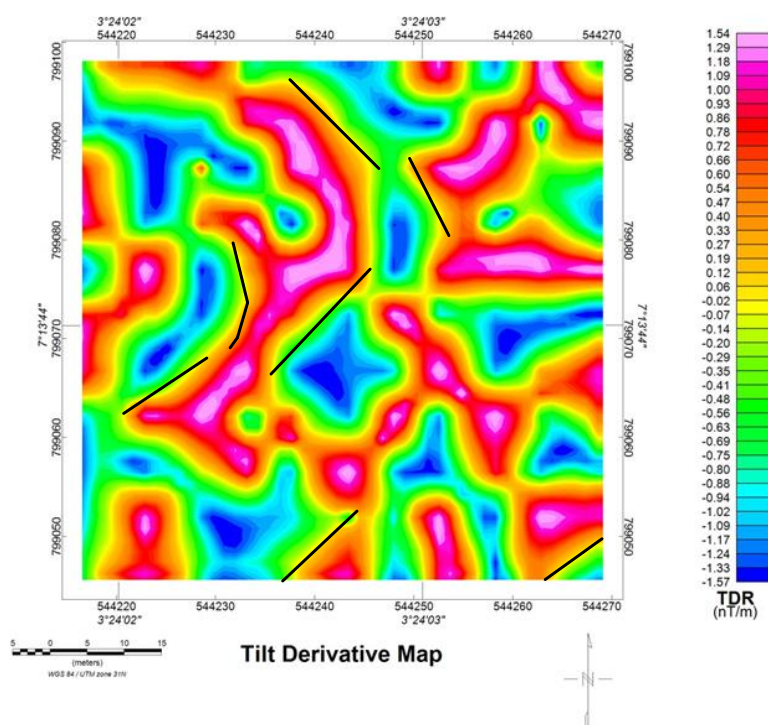


Figure 12. Tilt derivative map of the magnetic field (lineament inferred map).

The derivative techniques described, which helped in producing the derivative grids, are to aid the interpretation of geologic boundaries and other linear features (entrapments) of interest (Ferreira et al., 2011); Verduzco et al., 2004). Lines inferred on these maps, where there are steep gradients and discontinuities are to make the linear features more visible.

Lineation of the study area was also mapped by an approach known as the Centre for Exploration Targeting (CET) grid analysis. The CET is a set of algorithms designed as a plugin attachment of the interpretation

software used (Oasis Montaj version, 8.4) based at the University of West Australia. The CET uses tilt derivative grids of the gravity and magnetic fields (Figures 11 and 12, respectively) for its computation and analysis, in order to identify structural complexity via texture analysis, lineation detection, lineation vectorization, skeletonization, and thresholding. The process involves plotting solutions as curves that are vectorised into lines (lines less than 10 m are discarded). The vectorised lineament map is presented in Figure 13.

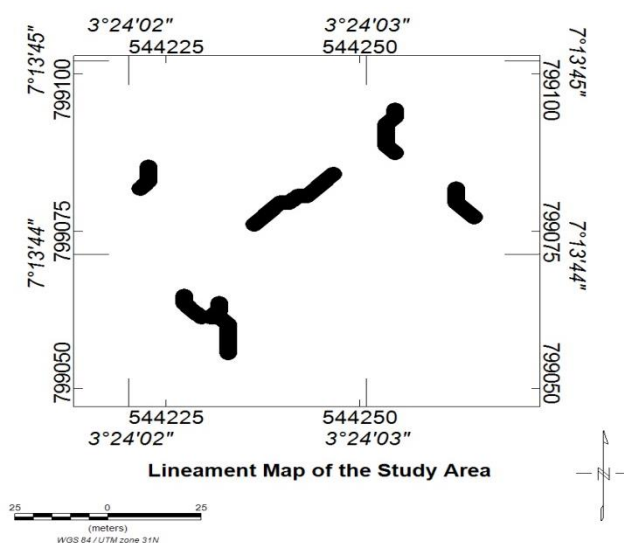


Figure 13. Lineament map of the study area (gravity field).

2-4. Quantitative Analysis (Depth Estimate)

In order to ensure the numerical analysis in this research, the Peter’s Half Slope Method (PHSM) and the 3D-Euler deconvolution method are employed.

The PHSM uses the profile’s half-maximum sloping flanks to estimate depths in potential field data interpretations (Peters, 1949; Nettleton, 1971; Rao & Babu, 1984; Telford et al., 1998; Milsom, 2003). According to Peters, the maximum slope distance (d) in meters is approximately equal to 1.6 h, where h is the depth to the potential source as presented in Figure 14.

Summarily, the technique involves locating the curve with maximum amplitude (most steep portion) on the magnetic intensity or Bouguer anomaly profile after plotting the corrected (reduced) gravity or magnetic values of each station point against its corresponding distance on Microsoft Excel. A straight line is drawn through the maximum slope, intersecting the x-axis of the

graph to produce a slope line. A vertical line to connect the maximum slope’s top end with the x-axis is drawn and measured with a meter rule, its middle point is marked. The half-slope line is then produced by drawing a straight line connecting the slope’s intersection with the x-axis and the middle point of the vertical line. Two straight lines parallel to the half-slope line and tangential to the Bouguer anomaly or magnetic intensity line are added, slightly touching the curve. Two new vertical lines, starting from the two points where the tangent lines touch the curve and ending at the x-axis, are drawn. The distance between these two vertical lines are measured and noted as distance. (These values are converted to ensure they are in agreement with the ground units as compared with the meter rule measurements). Each potential source body solved for are assigned an index value (Structural Index, SI), ranging from 1.2 to 2.0. The graphs of selected profiles of both gravity and magnetic field are presented in Figures 15 to 18.

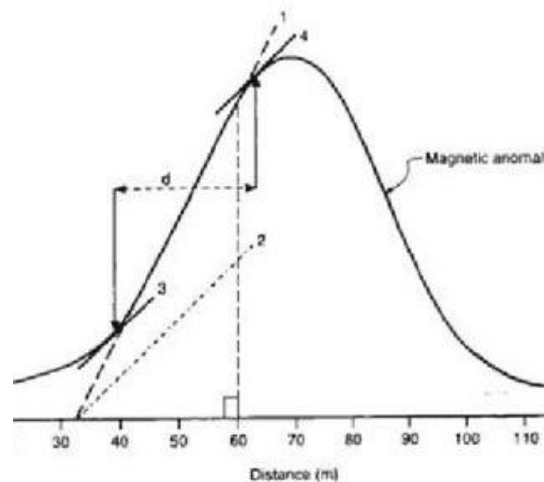


Figure 14. Peters’ Half Slope Method (PHSM) of Depth to Sources Determination (Telford et al., 1998).

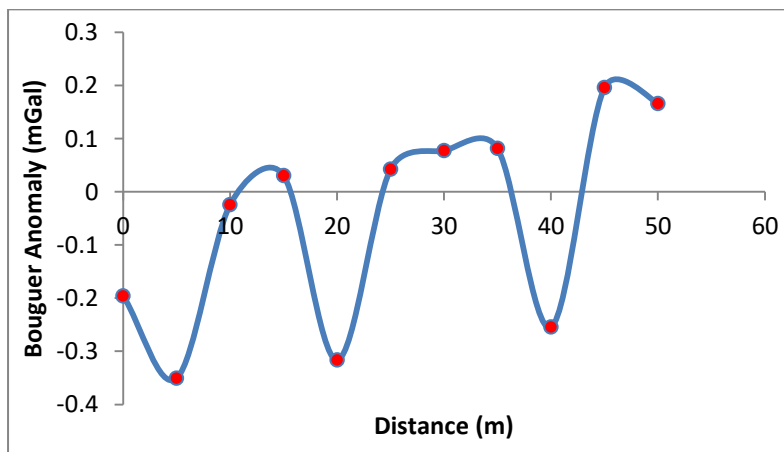


Figure 15. Graph of corrected gravity data on Profile 1.

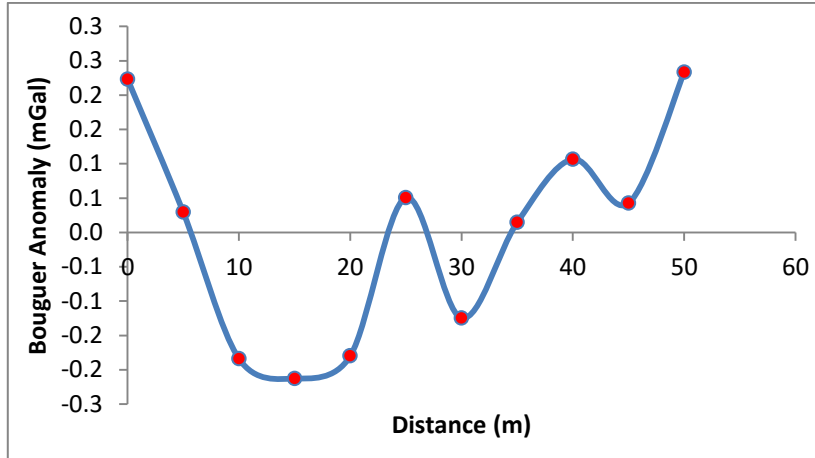


Figure 16. Graph of corrected gravity data on Profile 3.

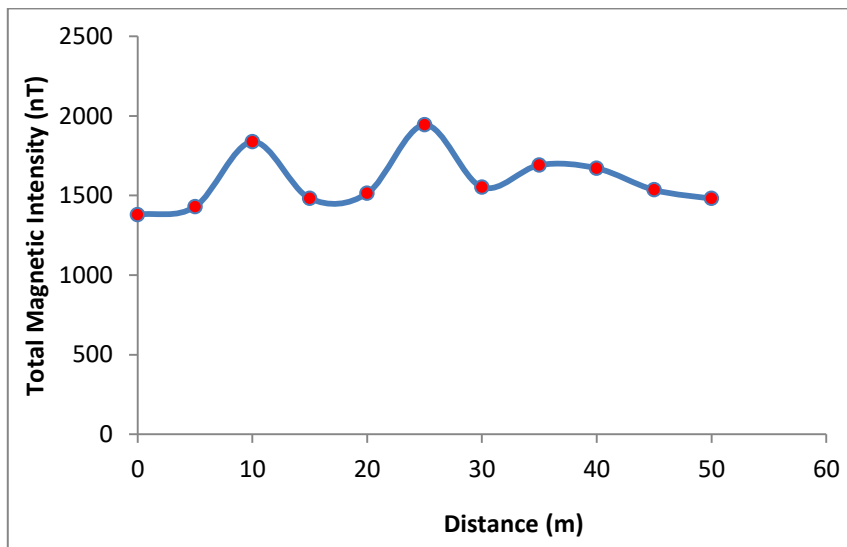


Figure 17. Graph of IGRF corrected magnetic data on Profile 3.

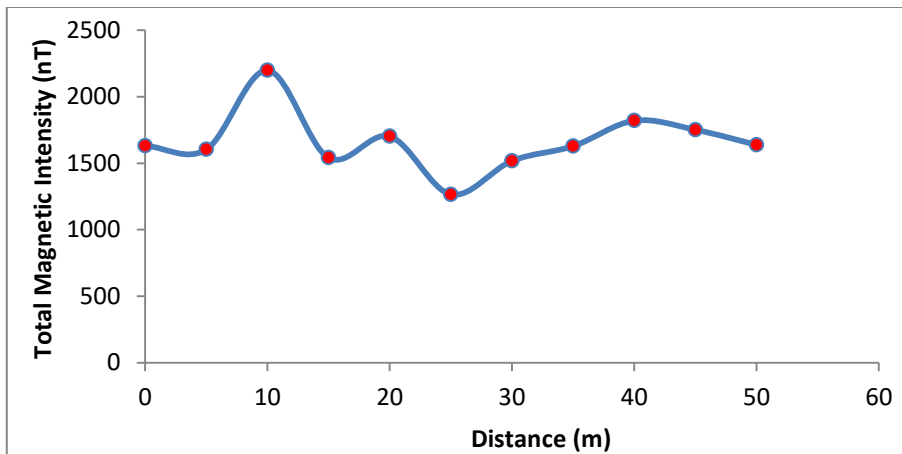


Figure 18. Graph of IGRF corrected magnetic data on Profile 3.

The following simple equation holds, for varying potential bodies, to find the depth of the object beneath.

$$d = 1.2h \quad (\text{for a very thin body}) \quad (4)$$

$$d = 1.6h \quad (\text{for a body of intermediate thickness}) \quad (5)$$

$$d = 2.0h \quad (\text{for a very thick body}) \quad (6)$$

Using the arithmetic explained above, an average is evaluated for profiles showing more than one anomaly after plotting. The average then becomes the depth representation of the profile. Similarly, the

average of the depths of each profile of gravity and magnetic field is calculated to represent the depth of gravity sources and magnetic sources, respectively. Tables 1 and 2 show the comprehensive results of the gravity and magnetic sources evaluated.

The 3-D Euler deconvolution method is premised on a system of linear equations called the 'homogeneity equation' that relates the potential field and its gradient components to the position of the source, with the degree of homogeneity η , which is interpreted as a structural index, SI (Thompson, 1982).

The 3-D form of Euler's equation can be defined mathematically as (Adegoke & Layade, 2019; Reid et al., 1990):

$$x \frac{\partial T}{\partial x} + y \frac{\partial T}{\partial y} + z \frac{\partial T}{\partial z} + \eta T = x_0 \frac{\partial T}{\partial x} + y_0 \frac{\partial T}{\partial y} + z_0 \frac{\partial T}{\partial z} + \eta b \quad (7)$$

where;

x, y and z are the coordinates of a measuring point; x_0 , y_0 and z_0 are the coordinates of the source location whose total field is detected at x, y and z; b is a base level; η is structural index (SI) and T is total potential field.

The method as developed by Thompson (1982) is based on functions governing potential field properties. The Euler deconvolution method was further developed

and generalized by Ravat (2007) to suite a wider range of source types (geologic structures). The structural index (SI) for different potential source geometries (geologic models) is summarized in Table 3. The total field grid (Figure 3 for gravity and Figure 4 for magnetic) with their respective directional derivative grids were used. The reviews of literature and existing knowledge of the geology of this research area were carefully guided in the choice of parameters such as the grid interval (cell size), window size, structural indices, maximum/minimum distance, x/y offsets, maximum % location tolerance (dXY) and maximum % depth tolerance (dZ). To minimize error in the depth computations and obtain the best possible results, dZ is set to 15%, dXY to 22%, x and y offset to ± 10 m while the SI 0.0 and 1.0 were used for gravity and magnetic field, respectively. The solution is plotted using the zone colored plot to have a 3D view of potential sources at varying depths. Although, other structural indices of gravity and magnetic were tried on the solution, SI =0.0 (gravity) and SI =1.0 (magnetic) were accepted to be the fairest solutions that represent the 3D Euler depth solutions of the study area, presented in Figures 19 and 20 (gravity); and Figures 21 and 22 (magnetic).

Table 1. Depth to Gravity Sources from PHSM.

Geologic structure (Profile)	Very thin (m)	Intermediate (m)	Very thick (m)	Average
1	5.52	7.36	9.20	7.36
2	5.78	7.68	9.60	7.69
3	11.04	14.72	18.40	14.72
4	5.26	7.04	8.80	7.03
5	6.24	8.32	10.40	8.32
6	5.28	7.04	8.80	7.04
7	8.40	11.20	14.00	11.20
8	11.04	14.72	18.40	14.72
9	5.28	7.04	8.80	7.04
10	5.76	7.68	9.60	7.68
11	10.08	13.44	16.80	13.44
Overall average	7.24	9.65	12.07	9.65

Table 2. Depth to Magnetic Sources from PHSM.

Geologic Structure (Profile)	Very thin (m)	Intermediate (m)	Very thick (m)	Average (m)
1	4.04	5.39	6.73	5.39
2	2.94	3.92	4.90	3.92
3	2.76	3.68	4.60	3.68
4	2.39	3.18	3.98	3.18
5	2.76	3.68	4.60	3.68
6	4.41	5.88	7.36	5.88
7	2.76	3.68	4.60	3.68
8	2.58	3.44	4.30	3.44
9	4.23	5.64	7.05	5.64
10	3.86	5.15	6.44	5.15
11	2.58	3.44	4.30	3.44
Overall average	3.21	4.28	5.35	4.28

Table 3. Structural Index for Geological Models. (Thompson, 1982; Telford et al. 1998).

Geological Model	Number of Infinite Dimensions	Gravity SI	Magnetic SI
Sphere	0	2	3
Pipe	1 (Z)	1	2
Horizontal Cylinder	1 (X or Y)	1	2
Dyke	2 (Z and X or Y)	0	1
Sill	2 (X and Y)	0	1
Contact	3 (X, Y and Z)	0	0

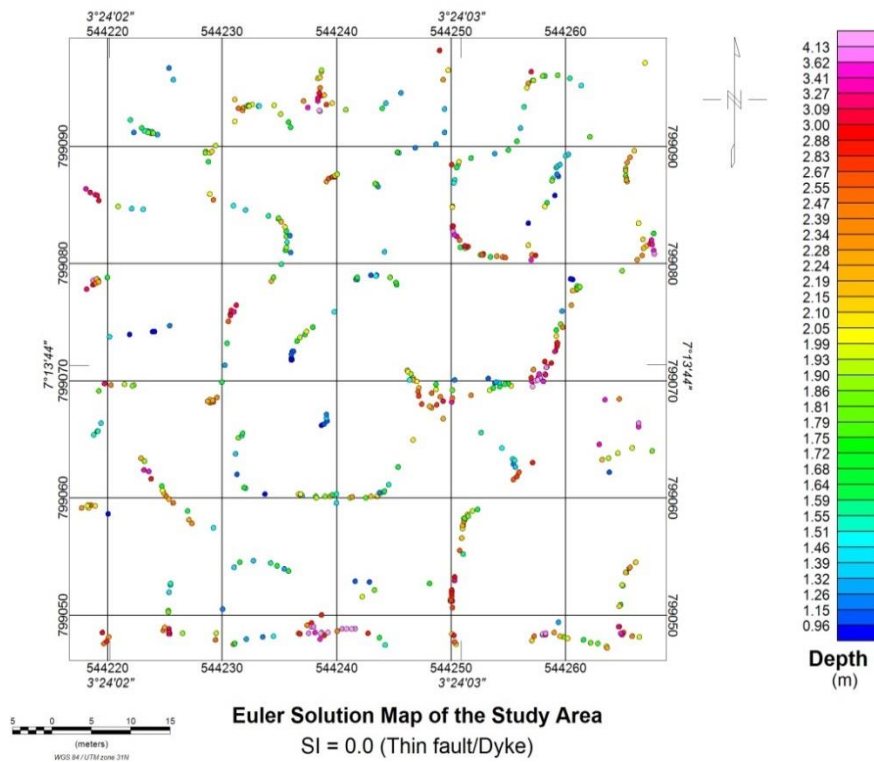


Figure 19. 3D Euler Solution Map of the Gravity Field (SI = 0).

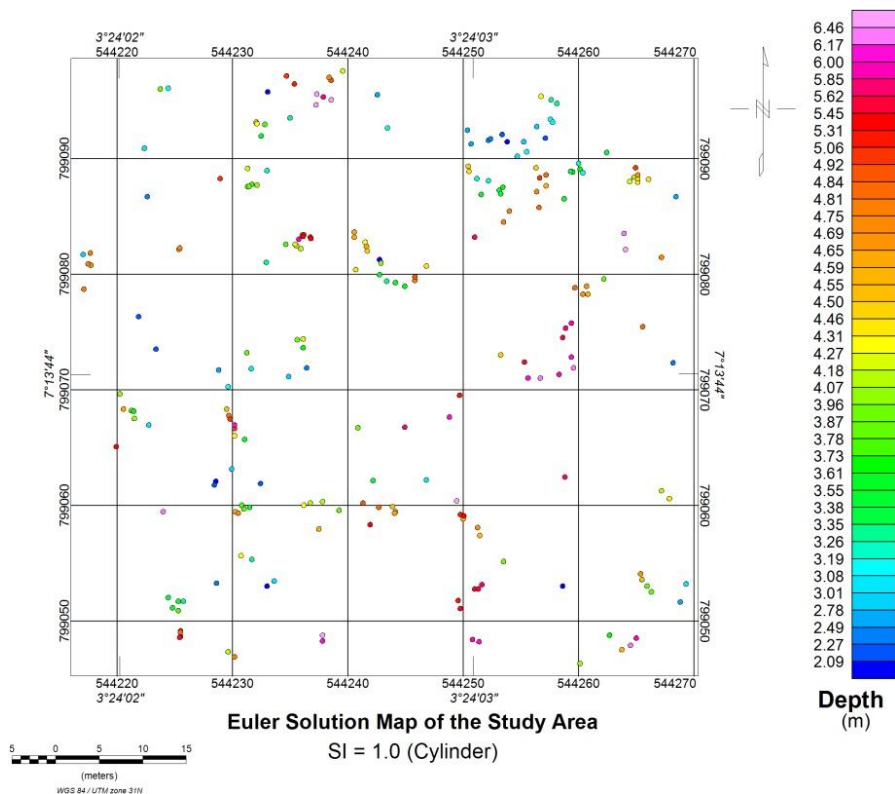


Figure 20. 3D Euler Solution Map of the Gravity Field (SI = 1).

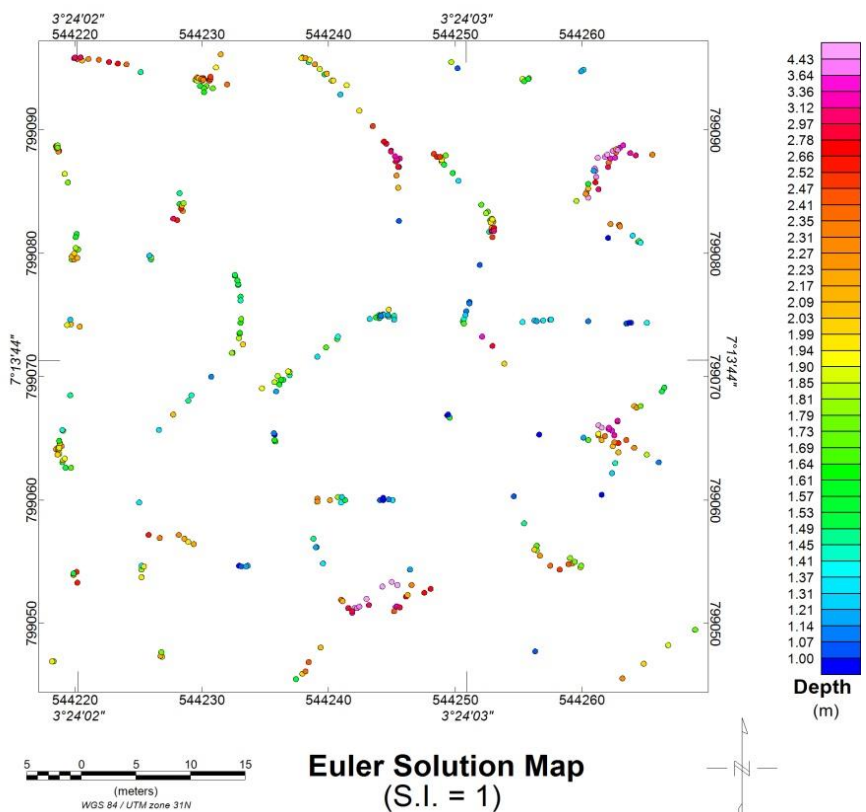


Figure 21. 3D Euler Solution Map of the Magnetic Field (SI = 1).

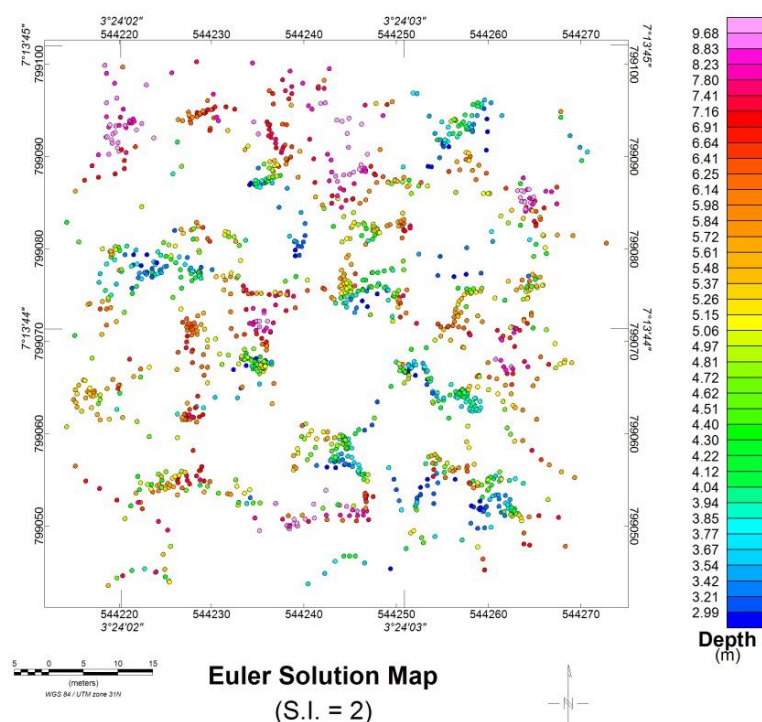


Figure 22. 3D Euler Solution Map of the Magnetic Field (SI = 2)

3. Discussion of Results

3-1. Discussion of Qualitative Results

The corrected values of each station's points of gravity and magnetic have been gridded to represent the total fields, presented in Figure 3 and Figure 4, respectively. Figure 3 shows the Bouguer gravity field with a gravimetric range of -0.68 to 0.66 mGal, revealing the distribution of high density bodies across the surveyed plot. The gravity field is affected by density contrasts caused by deep-seated anomalies (regional structures) and shallow-placed signals (residual responses) (Essa et al., 2018). A decrease in the gravity values is observed from the west through the east of the area. The high density zones are characterized by green, yellow, red and pink coloration with a Bouguer anomaly range of about -0.02 to 0.66 mGal. The negative and low Bouguer gravity values suggest the presence of low density rock units that are possibly alluvium deposits compacted into the entrapments (lineaments) identified in the area. The total magnetic intensity of the area represented in Figure 4 shows basement variations as a result of differences in the magnetic values ranging from 603 to 2837 nT. The grid shows the dominance of high magnetic amplitudes spread all over, with a few patches of low magnetic values around the central and eastern parts of the study area.

The presence of these high magnetic values predicts the presence of igneous or metamorphic rock units, as also shown in Figure 1 that is the geological map of the study area.

The reduced gravity field produced the residual anomaly map (Figure 7) after applying a Gaussian filter at 0.00025 cycles per meter. The residual grid of the gravity revealed a range of -0.57 to 0.61 mGal, the disappearance of some low-frequency anomalies around the northwestern corner of the grid as compared to the Bouguer gravity field (Figure 3) is as a result of the filtering process employed that has attenuated regional anomalies obscuring signals. The Residual Magnetic Intensity (RMI) map is a result of IGRF subtracted from the total magnetic intensity of the area, displayed in Figure 8, with an amplitude range of -897 to 905 nT. The negative magnetic value range of -891 to -6 nT is seen to be sparsely distributed on the grid, which connotes that the area is composed of magnetically susceptible contents.

The horizontal directional derivative along the X-direction (Figure 9) for the gravity revealed -0.223 to 0.217 mGal/m as its range of values, and -339.06 to 409.07 nT/m is the range of values for the horizontal directional derivative along the Y-direction for the

magnetic. Tilt derivative grid evaluated from the gravity field has a range of values of -1.533 to 1.536 mGal/m, while the corresponding magnetic tilt derivative shows a range of -1.57 to 1.54 nT/m. The positive values of these derivative grids are associated with the peak signals, which predict the assemblage of gravity and magnetic bodies. Steep discontinuities and continuous elongation of contours, as shown by inferred strokes (lines) on the tilt derivative maps, revealed a wide range of linear structures. The general trends of all the derivative grids are northeast (NE) and southwest (SW), as seen from the selected ones (Figures 9 to 12), similarly confirmed by the CET lineament map (Figure 13). This trend is in conformity with the Pan-African structural trends (Kaki et al., 2013).

3-2. Discussion of Depth to Sources' Results

The PHSM depth results of each gravity and magnetic profile have been detailed in Tables 1 and 2. The average range of depth to gravity sources, as estimated by PHSM, is 5.26 to 11.04 m for very thin bodies, 7.04 to 14.72 m for body of intermediate thickness and 8.80 to 18.40 m for very thick body, but with an overall average gravity depth of 9.65 m representing the average depth to gravity sources of the entire area. Similarly, the evaluated PHSM average depth to magnetic sources is 2.39 to 4.41 m using SI, corresponding to a very thin body, 3.18 to 5.88 m for an intermediate thickness body and 3.98 to 7.36 m for a very thick body. 4.28 m is the overall average depth of magnetic sources.

Figures 19 and 20 present the 3D Euler solution map of depth to gravity sources of $SI = 0$ and $SI = 1$, respectively. The results of the solution of $SI = 0$ for gravity and $SI = 1$ for magnetic were only accepted after using other SI in the computations, as these structural indices gave the fairest results in depth evaluation and lineation. Figure 19 (magnetic Euler solution map of $SI = 0$) reveals a minimum depth range of 0.96 to 1.55 m at 1.26 m average and a maximum depth range of 3.0 to 4.13 m averaged at 3.57 m average. The accepted result of Euler depth to magnetic sources (figure 21) showed a minimum depth range of 1.0 to 1.41 m at 1.21 m average, while its maximum depth

range is 2.97 to 4.43 m at 3.7 m average. The minimum depth ranges correspond to the depth locations of short wavelength anomalies of gravity or magnetic responses. Similarly, the maximum depth ranges reveal the depth locations of low frequency anomalies of gravity or magnetic signatures. The continuous elongation of contours observed on the Euler maps has direct implications for the predicted linear structures in the study area. The thickness of the sedimentary cover, as can be observed from the Euler results of both methods, is seen to increase from east to west of the study area.

4. Conclusion

Gravity and magnetic methods of geophysical survey have yet again proved very useful in environmental studies. The qualitative analysis of ground gravity and magnetic data revealed contrasting variations of underlying rocks in the basement. Steep gradients and discontinuities observed on most of the qualitative maps possibly suggest the linear structures below the subsurface of the research location, and these are interpreted as conduits or traps for mineral rocks accumulation. The depth, position and orientation of potential signatures (gravity and magnetic sources) have been mapped quantitatively and the range of depth results obtained clearly show that the study is composed of shallow depth intrusive mineral rocks. The results of both geophysical methods are very good, but the gravity results seem to be better in terms of geological boundaries and contacts. This may be due to the fact that the magnetic method depends solely on Earth's magnetic field, while the gravity method investigates the nature of the earth beneath by relating gravitational fields to density contrasts (Kevin, 1997; Nicholas, 2007). That is, gravity method can map both ferrous and non-ferrous rock units. The qualitative results of this research, viz-a-viz orientation of fault lines, lithology and geologic Formation are in agreement with the works of Olurin et al. (2015); Layade et al. (2020); Layade et al. (2021) and Edunjobi et al. (2021).

Generally, the average depth results obtained are around the grid distance (station interval), which explains the differences of depths resulted from previous researches in the area.

Acknowledgment

The authors appreciate the authority of the University and other collaborators in using the site for the research work

Competing Interests

The authors declared that there were no competing interest for this research

Funding

The authors were solely responsible for all the expenses of the research

References

- Abdelrahman, E.M., & Essa, K. S. (2015). Three least-squares Minimization Approaches to Interpret Gravity Data Due to Dipping Faults. *Pure and Applied Geophysics*, 172, 427-438.
- Adegoke, J. A., & Layade, G. O. (2019). Comparative depth estimation of iron-ore deposit using the Data-Coordinate Interpolation Technique for airborne and ground magnetic survey variation. *African Journal of Science, Technology, Innovation and Development (AJSTID)*, 11(5), 663-669. doi: 10.1080/20421338.2019.1572702.
- Adejuwon, B. B., Salami, A.A., Omatola, P.S., Ashien, S.O., Adeyemo, B.K., & Ujubonu E.G. (2018). Integrated EM (VLF) and Gravity Survey for the Delineation of Mineralized Veins in Touzuwa Area of Benue State. *International Journal of Engineering Research and Technology*, 7(2), 49 – 54.
- Akinse, A.G., & Gbadebo, A.M. (2016). Geological mapping of Abeokuta Metropolis.
- Anudu, G.K., Oluba, L.N., Onwuemesi, A. G., & Ikpokonte, A.E. (2012). Analysis of Aeromagnetic Data over Wamba and its Adjoining Areas in North-central Nigeria. *Earth Science Research Journal*, 16(1), 25-33.
- Araffa, S. A. S., El-bohoty, M., Abou Heleika, M., Mekkawi, M., Ismail, E., Khalil, A., & Abd El-Razek, E. M. (2018). Implementation of Gravity and Magnetic Methods to delineate the subsurface structural features of the basement complex in Central Sinai Area, Egypt. *NRIAG Journal of Astronomy and Geophysics*, 7, 162-174, Cambridge University Press.
- Cornford, C. (1990). Source Rocks and Hydrocarbons of The North Sea. In Glennie, K.W. (ed.) *Petroleum Geology of the North Sea. Basic Concepts and Recent Advances. Blackwell Science, Oxford*, 376-462.
- Dow, W.G. (1978). Petroleum Source Beds on Continental Slopes and Rises (2). *American Association of Petroleum Geologists (AAPG) Bulletin*, Vol. 62.
- Edunjobi, H. O., Layade, G. O., Falufosi, M. O., & Olurin, O. T. (2021). Lineament and Depth Evaluation of Magnetic Sources in a Geological Transition Zone of Abeokuta and its Environs, Southwestern Nigeria. *Pet & Coal*, 63(2), 548-560.
- Essa, K.S., Nady, A.G., Mostafa, M.S., & Elhussein, M. (2018). Implementation of Potential Field Data to depict the Structural Lineaments of the Sinai Peninsula, Egypt. *Journal of African Earth Sciences*, 147, 43-53.
- Essa, K. S., & Munsch, M. (2019). Gravity Data Interpretation using the Particle Swarm Optimization Method with Application to Mineral Exploration. *J. Earth Syst. Sci.*, 128:123; DOI:doi.org/10.1007/s12040-019-1143-4.
- Falufosi, M.O., & Osinowo, O.O. (2021). Evaluation of Basement Topography and Structures in the Dahomey Basin and Surrounding Environs of Southwestern Nigeria, using Satellite Gravity Data. *NRIAG Journal of Astronomy and Geophysics*, 10(1), 333-346.
- Ferreira, F. J. F., de Castro, L. G., Bongioiolo, A. B. S., de Souza, J., & Romeiro, M. A. T. (2011). Enhancement of the Total Horizontal Gradient of Magnetic Anomalies using Tilt Derivatives: Part II—Application to real data: *81st Annual International Meeting, SEG, Expanded Abstracts*, 887–891.
- Gluyas, J., & Swarbrick, R. (2005). *Petroleum Geoscience. Blackwell Science, Oxford*, 358pp.
- Hesham, S.Z., & Hesham, T.O. (2016). Application of High-Pass Filtering Techniques on Gravity and Magnetic Data of the Eastern Qattara Depression Area, Western Desert, Egypt. *National Research Institute of Astronomy and Geophysics*, 5, 106-123.
- Jones, H.A., & Hockey, R.O. (1964). The

- Geology of Parts of Southwestern Nigeria. *Bull. Geological Survey Nigeria*, 31, 101–102.
- Joshua, E.O., Layade, G.O., & Adeyemi, S.A. (2017). On the use of Linear Trend Analysis in Removing Regional Gradient from Ground Magnetic Data for Qualitative Interpretation. *Scholars Research Library, Archives of Physics Research*, 8(1), 4-10.
- Kaki, C., d'Almeida, G.A.F., Yalo, N. & Amelina, S. (2013). Geology and Petroleum Systems of the Offshore Benin Basin (Benin). *Oil & Gas Science and Technology- Rev. IFP Energies nouvelles*, 68(2), 363-381.
- Kevin, M. (1997). Gravity method overview. *Department of Geosciences, Southwest Missouri State University, Springfield, MO 65804*.
- Layade, G.O., Edunjobi, H.O., Makinde, V., N. Bada, B.S. (2020). Application of Forward and Inverse Modelling to High Resolution Data for Mineral Exploration. *International Journal of Earth and Space Physics*. DOI: 10.22059/JESPHYS.2020296560.1007192.
- Layade, G.O., Edunjobi, H.O., Makinde, V., & Bada, B.S. (2020). Ground Based Gravimetric for the Detection and Depth Mapping of Subsurface Geological Structures of Ilesha, Southwest Nigeria. *Journal of Earth and Space Physics*, DOI:10.22059/JESPHYS.2020.301010.1007209.
- Milsom, J. (2003). *Field geophysics*. 3rd Edition John Wiley and Sons Ltd, London, 232 pp.
- Nabighian, M. N., & Hansen, R. O. (2005). Unification of Euler and Werner deconvolution in three dimensions via the generalized Hilbert transform, *Geophysics*, 66.
- Nettleton, L.L. (1971). Elementary Gravity and Magnetics for Geologists and Seismologists: *Society of Exploration Geophysicists Monograph Series*, No 1, 83-87.
- NGSA (2005). Nigeria Geological Survey Agency (NGSA). Geological Map of Nigeria.
- Obaje, N.G. (2009). Geology and mineral resources of Nigeria. *Lecture Note in Earth Science*.
- Paterson, N.R., & Reeves, C.V. (1985). Applications of gravity and magnetic surveys: the state-of-the-art in 1985. *Geophysics*, 50, 2558-94.
- Peters, L.J. (1949). The direct approach to magnetic interpretation and its practical application. *Geophysics* 14, 290-320s.
- Rahaman, O. J. (1976). *Review of Basement Geology of Smith*, Western Nigeria.
- Rao, D.A., & Babu, H.V.R. (1984). On the Half-Slope and Straight-Slope Methods of Basement Depths Determination. *Geophysics*, 49, 1365–1368.
- Ravat, D. (2007). Reduction to Pole. *Encyclopedia of Geomagnetism and Paleomagnetism*, D. Gubbins and E. Herrero-Bervera (eds.), *Springer*, 856–857.
- Reid, A.B., Allsop, J.M., Granser, H., Millett, A.J., & Somerton, I.W. (1990). Magnetic Interpretation in Three Dimensions using Euler Deconvolution. *Geophysics*, 55, 80-99.
- Reid, A.B., Ebbing, J., & Webb, S.J. (2012). Egregious Euler Errors – The Use and Abuse of Euler Deconvolution applied to Potential Fields. *74th EAGE Conference and Exhibition incorporating SPE EUROPEC 2012*, Copenhagen, Denmark, 4-7, June 2012.
- Telford, W. M., Geldart, L. P., Sheriff, R. E., & Keys, D. A. (1976). *Applied Geophysics*: Cambridge Univ. Press, NY, 1-860.
- Telford, W.M., Geldart, L.P. and Sheriff, R.E. (1998). *Applied Geophysics*, 2nd Edition, *Cambridge University Press*, USA 770 pp.
- Thompson, D. T. (1982). A new technique for making computer-assisted depth estimates from magnetic data. *Geophysics*, 47(1), 31-37.
- Verduzco, B., Fairhead, J. D., & Green, C. M. (2004). New Insights into Magnetic Derivatives for Structural Mapping. *The Leading Edge*, 23(2), 116–119.
- Webring, M. (1981). MINC. A Gridding Programme based on Minimum Curvature. *U.S Geological Survey Open-File Report*, 81-1224, 43p.
- Wright, J.B., Hastings, D.A., Jones, W.B., & Williams, H.R. (1985). *Geology and Mineral Resources of West Africa*, *George Allen and Urwin*, London, 90-120.